広島大学学位請求論文

Human-biased *TMEM25* expression promotes expansion of neural progenitor cells to alter cortical structure in the developing brain

(大脳皮質発達における *TMEM25* のヒト特異的発現レベル制御による神経幹細胞の増殖促進と層構造変化)

２０２３年広島大学大学院統合生命科学研究科

生命医科学プログラム

Boyang An

目次

主論文

Human-biased *TMEM25* expression promotes expansion of neural progenitor cells to alter cortical structure in the developing brain

(大脳皮質発達における *TMEM25* のヒト特異的発現レベル制御による神経幹細胞の増殖促進と層構造変化)

CONTENTS

Abstract

Cortical expansion has occurred during human brain evolution. Accumulating evidence indicates that human-specific genes underpin cortical expansion by diversifying the number of neural progenitors (NPCs), whereas many more conserved genes showing biased expression between species should also play crucial roles in this process. By comparing human and mouse RNA-seq datasets, I found that a conserved gene, transmembrane protein 25 (*TMEM25*), was much more highly expressed in human NPCs. Overexpression of either human *TMEM25* or mouse *Tmem25* similarly promoted proliferation of mouse cortical progenitors in vitro. Mimicking human-type expression of *TMEM25* in mouse ventricular cortical progenitors accelerated proliferation of basal radial glia (bRG) (cells specifically and abundantly distributed in human subventricular zone [SVZ]) and increased the number of upper-layer neurons in vivo. By contrast, RNA-seq analysis and pharmacological assays showed that knockdown of *TMEM25* in cultured human NPCs compromised the effects of extracellular signals, leading to cell cycle inhibition via Akt repression. These data suggest that *TMEM25* can receive extracellular signals to expand bRG, a process which occurs specifically in human cortical development.

Keywords: *TMEM25*, human cortical development, neural progenitor cells, proliferation

Introduction

Homo sapiens stands apart from other mammals due to advanced cognitive abilities, which are closely linked to expansion of the neocortex (Ncx) [1-3]. The size of the Ncx is largely determined by the proliferative capacity of neural progenitors (NPCs) [1,4-6]. NPCs in the developing Ncx are mainly divided into two classes: apical progenitors (APs) and basal progenitors (BPs). While APs exhibit high levels of proliferation in most mammalian species, BPs have been found to display significant differences in proliferative capacity [7,8]. In species with lissencephalic Ncx, such as mouse, about 90% of BPs are basal intermediate progenitors (bIPs). These bIPs undergo division once, generating two neurons [9-11]. In contrast, in species with gyrencephalic Ncx, such as human, about 50% of BPs are basal radial glia (bRG) that undergo several division cycles to generate future BPs [1,12]. This leads to the production of a large number of BPs, resulting in the expansion of a part of the subventricular zone (SVZ), called the outer SVZ [13,14]. Currently, some human- and/or primate-specific genes responsible for Ncx expansion have been reported, such as *TMEM14B, NOTCH2NL* and *TBC1D3* [2,15-17]. It is noteworthy that, as cortical folding has developed gradually during evolution, it is most likely that multiple well-conserved genes are also involved in human BPs expansion.

The transmembrane protein (TMEM) family belongs to the immunoglobulin superfamily and TMEM proteins have been found to span biological membranes. Several studies have demonstrated that TMEM members are involved in various physiological processes such as proliferation and apoptosis by modulating intracellular signal transduction pathways [18-20]. *TMEM* family genes include *TMEM14B*, a primate-specific gene, as mentioned earlier, that plays a crucial role in regulating proliferation of BPs by promoting G1/S transition, leading to cortical expansion and folding [15]. I

hypothesized that other TMEM family genes exhibit similar potentials to play roles in cortical development in human-specific manners.

Here, I show from a comparison of RNA-seq data between humans and mice that *TMEM25* shows significantly higher expression levels in human NPCs than in mice. At present, *TMEM25* is utilized as a biomarker for breast and colorectal cancer [21]. In the context of brain development, it is worth noting that *TMEM25* is involved in the regulation of neuronal excitation and epileptogenesis [22]. Since abnormal proliferation, followed by deregulated differentiation of neurons, causes epilepsy [23], it seems likely that *TMEM25* may also regulate NPC behaviors. In the present study, I manipulated the level of *TMEM25* in vitro and in vivo to test the hypothesis that a conserved TMEM family gene can be responsible for differentiating the modes of cortical expansion and development depending on its expression level.

Materials and Methods

Animals

All aspects of animal treatment and care were performed in line with the guidelines of the Experimental Animal Care Committee of Hiroshima University (Higashi-Hiroshima, Japan). Timed pregnant ICR mice (Japan SLC) were used in this study.

Cell culture

Mouse NPCs were isolated from E14.5 mice (female and male) according to a previously described protocol [50]. In brief, the embryo telencephalons were triturated in Hanks' balanced salt solution (HBSS) by gentle pipetting. After centrifugation, dissociated cells were resuspended in N2-supplemented Dulbecco's Modified Eagle Medium (DMEM) /F-12, supplemented with 10 ng/ml basic fibroblast growth factor (bFGF) and 10 ul/ml penicillin/streptomycin/fungizone (PSF) and plated on dishes coated with poly-L-ornithine and fibronectin.

Human NPCs (AF22 cell line) were cultured in hN2 medium supplemented with 10 ul/ml PSF, 10 ng/ml EGF, 10 ng/ml bFGF and 10 ul/ml B27 and plated on dishes coated with poly-L-ornithine and laminin. The cells were passaged at a ratio of 1: 2 every third or fourth day using TrypLE Select.

For the rescue experiment, the Akt activator SC79 (5 μg/ml; Selleck), Akt inhibitor VIII (5 μg/ml; Merck) were added one day after infection. For detecting downstream signalings, cells were cultured in DMEM /F-12 without growth factors overnight. Following starvation, the cells were treated with 10 ng/ml EGF for 20 min.

Constructs

Lentivirus vectors used to express FLAG-tagged MeCP2 (pLEMPRA) and short-hairpin RNAs (shRNAs; pLLX) were provided by Dr. Z. Zhou (University of Pennsylvania School of Medicine, Philadelphia, PA, USA) and Dr. M. E. Greenberg (Harvard Medical School, Boston, MA, USA) [51,52]. A FLAG-tagged mouse and human expression lentivirus vector was constructed by replacing MeCP2 with *TMEM25* at the EcoRI and AscI sites of pLEMPRA-MeCP2. shRNAs against *TMEM25* and panc*TMEM25* were designed to target human genes.

Lentivirus production

Lentiviruses were produced as described previously [50]. Briefly, lentivirus particles were generated by co-transfecting HEK293T cells with the lentivirus constructs pCAG-HIVgp and pCMV-VSV-G-RSV-Rev using polyethyleneimine (PEI). The culture supernatants were collected 48 h after transfection, and virus was introduced into human and mouse NPCs by adding supernatants to the culture medium.

qRT-PCR analysis

Total RNA was isolated with Sepasol-RNA I Super G and subjected to reverse transcription with the ReverTra AceTMqPCR RT Master Mix with gDNA Remover kit, according to the manufacturer's instructions. qRT-PCR was performed using a THUNDERBIRD Next SYBR qPCR Mix Kit with ROX as the reference dye using the CronoSTARTM 96 Real-Time PCR System. The expression levels of each gene were normalized to that of GAPDH and calculated relative to that of the control. PCR primers used in this study are listed in Table 1.

In utero electroporation

Timed pregnant mice at E13.5 were anaesthetized. Plasmid DNA (1.0 ug/ml) containing 0.1% Fast Green was injected into the lateral ventricle of the embryonic brain from outside the uterus using a calibrated glass micropipette. For electroporation, 50-msec electric pulses of 45 V were delivered five times at intervals of 950 ms using a Super Electroporation NEPA21 Type II. After the procedure, the uterus was placed back in the abdominal cavity and the wound was surgically sutured. Embryonic brains were perfused with 4% paraformaldehyde at E15.5 or E18.5. Then, fixed brains were dehydrated in 10% and 20% sucrose in PBS at 4 ºC sequentially.

Immunocytochemistry

Cells were fixed with 4% paraformaldehyde and washed with PBS. Cells or embryonic brain sections were permeabilized and blocked with blocking buffer (3% FBS and 0.1% Triton X-100 in PBS) for 20 min at room temperature and then incubated with primary antibodies overnight at 4 ºC. The following primary antibodies were used: chick anti-GFP (1:500; Aves labs, GFP1020); rabbit anti-active caspase3 (1:500; R&D, AF835); rabbit anti-Pax6 (1:500; Biolegend, PRB-278P); mouse anti-phospho-histone H3 Ser10 (1:500; CST, 9706S); goat anti-Sox2 (1:500; R&D, AF2018); rabbit anti-Tbr2 (1:500; Abcam, ab23345); mouse anti-Satb2 (1:500; Abcam, ab51502); rat anti-Ctip2 (1:500; Abcam, ab18465). After cells or slices were washed three times with PBS, they were incubated for 2 h at room temperature with corresponding secondary antibodies: CF488A donkey anti-chicken IgY (IgG) (H＋L), highly cross-adsorbed (1:500; Biotium); CF555 donkey anti-goat IgG (H＋L), highly cross-adsorbed (1:500; Biotium); CF555 donkey anti-mouse IgG (H＋L), highly cross-adsorbed (1:500; Biotium); CF555 donkey anti-rabbit IgG (H

＋L), highly cross-adsorbed (1:500; Biotium); CF568 donkey anti-rat IgG (H＋L), highly cross-adsorbed (1:500; Biotium); CF647 donkey anti-rabbit IgG (H＋L), highly cross-adsorbed (1:500; Biotium); or CF647 donkey anti-mouse IgG (H＋L), highly cross-adsorbed (1:500; Biotium). Hoechst 33258 (1:500; Nacalai Tesque, 04928-92) was used for nuclear staining. After the sections were washed three times with PBS, they were mounted on glass slides with Immu-Mount (Thermo Scientific).

EdU assays

Cells were cultured with 10 uM EdU in Click-iT EdU Imaging Kits for 30 min, fixed with 4% PFA, permeabilized with 0.1% Triton-X and 3% FBS in PBS, and stained with Click-iT reaction buffer at room temperature for 1 h in the dark. After washing with PBS, primary and secondary staining were performed in the dark.

RNA sequencing and data analysis

RNA sequencing was performed using the Illumina Hiseq® 2500 system (Illumina, San Diego, CA, USA) as described previously [25]. Adaptor and incomplete sequences were removed by Trim Galore. Short-read sequences were mapped on the human reference genome hg38 by STAR [53]. Mapped reads were counted by BEDTools [54]. To compare gene expression changes, I utilized TPM values.

Western blotting

Proteins were extracted using RIPA buffer (Thermo Scientific) with 1% protease inhibitor (Nacalai Tesque), separated by SDS-PAGE and transferred onto PVDF membranes (Millipore). Then, the membranes were cut to separate proteins according to molecular mass and blocked with 5% skim milk at room temperature for 1 h. The membranes were

incubated with primary antibody overnight at 4 °C. The following primary antibodies were used: phospho-Akt (1:2000; CST, 4060); Akt (1:1000; CST, 9272); phospho-Creb (1:1000; CST, 9198); Creb (1:1000; CST, 9197); phospho-p53 (1:1000; CST, 9284); p53 (1:1000; CST, 9282); GAPDH (1:1000; CST, 5174). After being washed three times with TBST, membranes were incubated at room temperature for 1 h with secondary antibodies. Immunoreactive bands were detected by enhanced chemiluminescence using Chemi-Lumi One Super (Nacalai tesque).

Quantification and statistical analysis

Experiments were conducted using at least three biological replicates for each group. Statistical analyses were performed using both Student's t test and Mann-Whitney U test for comparisons between two groups, or one-way ANOVA with post hoc LSD or Tukey-Kramer test for multiple groups comparison. Exact values of n (sample size) are provided in the figures and figure legends. For cell counting, three or more different areas were chosen in each sample of any groups to avoid biased measurement. All data are presented as mean ± standard error of the mean (SEM). Statistical significance was set at p-value less than 0.05.

Results

TMEM25 was more highly expressed in human neocortex compared to mouse neocortex

To identify *TMEM* genes showing higher expression during human brain development, I first analyzed published RNA-seq data to compare human and mouse NPCs derived from developing Ncx [24]. A heatmap showed that various genes belonging to the TMEM family were variably expressed in apical radial glia (aRG) and bRG of humans compared with those of mice (Fig. 1A). Next, I searched for genes expressed at least two-fold more highly in human progenitor cells than in mice progenitor cells (61 genes). I then narrowed the scope by detecting whether promoter-associated non-coding RNAs (pancRNAs) [25-27] that can potentially activate the partner *TMEM* genes were expressed using the public RNA-seq data of AF22 (Fig. 1B) [28]. I found that *TMEM25*, *TMEM51*, *TMEM18*, *TMEM159* and *TMEM220* pancRNA-partnered genes were biasedly expressed in human aRG/bRG (Fig. 1C). Among them, *TMEM25* showed the highest similarity with mouse *Tmem25* at the protein level (91.88%: Fig. 1D). I also compared published RNA-seq data from human and mouse VZ and SVZ [29]. Compared to the levels in mouse, the levels of *TMEM25* were significantly increased in both human VZ and SVZ (Fig. 1E). Thus, *TMEM25* was selected for the following experiments

TMEM25 was necessary for NPC proliferation

To investigate the effect of *TMEM25* on proliferation of human NPCs, I performed knockdown of *TMEM25* in a human iPSC-derived NPC line, AF22 (Fig. 2A,B). I immunostained incorporated 5-ethynyl-2′ -deoxyuridine (EdU) to monitor the cell cycle progression. I found that *TMEM25* knockdown decreased EdU+ cells by approximately

half, compared to the control group (Fig. 2C,D), indicating that *TMEM25* functions in the proliferation of NPCs. qPCR analysis showed that knockdown of *TMEM25* dramatically decreased the mRNA level of a proliferation marker, Ki67 encoded by *MKI67* gene, and a stem cell marker, *SOX2* gene (Fig. 2E,F), indicating that *TMEM25* functions in maintenance of the stemness of NPCs.

I further examined the effect of *TMEM25* on cell survival by immunostaining active Caspase3. As shown in Fig. 3A,B, the percentage of active Caspase3+ cells was not altered after *TMEM25* knockdown. Taken together, my data indicate that *TMEM25* is necessary for NPC proliferation, but not for NPC survival.

Expression level of *TMEM25/Tmem25* determined proliferation rate of mouse NPCs

Even though *Tmem25* was expressed in the mouse NPCs at a very low level, it was still possible that difference(s) in the protein structures of *TMEM25/Tmem25* caused differential NPC behaviors. Therefore, I overexpressed either *TMEM25* or *Tmem25* in mouse NPCs prepared from embryonic day (E) 14.5 forebrains. As shown in Fig. 4A,B, regardless of which ortholog was expressed, the overexpression significantly increased EdU+ cells under proliferation conditions, strongly suggesting that the difference in the expression level rather than in the sequence of these orthologs is the key to determining the proliferation rate of NPCs.

Human *TMEM25* expression promoted cortical development through increasing bRGs

To explore potential roles of *TMEM25* in neural development, I induced human *TMEM25* expression together with GFP expression in mouse lateral ventricles on E13.5 by *in utero*

electroporation. At E15.5, I performed phosphorylated Histone H3 (PH3) staining to evaluate the effect of *TMEM25* on NPC proliferation in the SVZ. As shown in Fig. 5A,B, *TMEM25* expression increased PH3+ cells, suggesting that it promoted generation of BPs.

Because two progenitor subtypes exist in the SVZ (bRG and bIPs), I similarly investigated which type of progenitor was affected by *TMEM25* expression. In addition to bIPs which are abundant in mice, I found GFP+ cells with a basal process [12] corresponding to bRG (Fig. 5C). Remarkably, I found that *TMEM25* expression caused an increase in Pax6+/GFP+ cells in the SVZ (Fig. 5D,E).

Consistently, there was also an increase in Sox2+ cells after *TMEM25* electroporation, indicating that *TMEM25* has the potential to increase generation of bRG (Fig. 6A,B). However, I observed that overexpression of *TMEM25* had little effect on the generation of Tbr2+ bIPs (Fig. 6A,C). Thus, *TMEM25* expression can promote derivation and subsequent proliferation of bRG.

Previous studies have shown that bRG frequently provide extra scaffolding for migration of neurons and typically undergo multiple rounds of cell division to generate the majority of upper layer neurons, which are younger than deep-layer neurons, to extend neurogenesis [15,30-32]. I next examined which type of neurons was affected by *TMEM25*. At E18.8, Satb2 (a marker for layer II/III neurons) and Ctip2 (a marker for layer V) immunostaining showed that *TMEM25* expression dramatically increased the number of upper-layer neurons, whereas it tended to decrease the number of deep-layer neurons (Fig. 7A-C). Taken together, these findings indicate that increased expression of *TMEM25* in mouse Ncx leads to an increase in the number of bRG, ultimately increasing the generation of upper-layer neurons.

TMEM25-knockdown human NPCs exhibited total downregulation of cell-cycle-related genes

To reveal the molecular mechanism by which *TMEM25* regulates neurogenesis, I performed RNA-seq to examine the transcriptome changes after *TMEM25* knockdown in human NPCs. I observed differentially expressed genes (DEGs), including 371 down-regulated genes and 162 up-regulated genes (Fig. 8A). Gene ontology analysis (GO) showed that the down-regulated genes were enriched in cell cycle (GO: 0007049), chromosome segregation (GO: 0007059) and cell division (GO: 0051301) genes (Fig. 8B), well supporting my data that EdU incorporation decreased after *TMEM25* knockdown (Fig. 2C,D). These findings clearly indicate that *TMEM25* plays a key role in NPC proliferation. The up-regulated genes were enriched in neuron development (GO: 0048666) and nervous system development (GO: 0007399) genes, suggesting that *TMEM25* knockdown alters NPC pools to provide more premature neurons, consistent with the previous research showing that deregulated *TMEM25* expression leads to epileptogenesis [22]. I looked at the expression of human-specific genes that have been shown to be involved in cortical expansion, and found that *ARHGAP11B* expression was specifically decreased in the *TMEM25* knockdown group, while other genes were not affected (Fig. 8C-E). Notably, overexpression of *ARHGAP11B* rescued inhibition of proliferation of NPCs caused by knockdown of *TMEM25* in human AF22 (Fig. 9A,B), suggesting a specific link between human-biased expression of *TMEM25* and the regulatory network governed by a human-specific gene. KEGG pathway analysis showed that down-regulated genes were enriched in cell cycle and p53 signaling pathways (Fig. 8F). Taken together, the findings indicate that *TMEM25* knockdown disturbed a human-specific molecular network to alter NPC proliferation.

***TMEM25* regulated cell cycle progression via Akt pathway in NPCs.**

To identify key downstream targets, I searched for hub genes by performing Protein-Protein Interaction Networks analysis (PPI). As shown in Fig. 10 and 11A, the top ten genes were displayed. Among them, I found two critical G2/M regulatory genes, *CDK1* and *CCNB1*, which control G2/M transition [33,34]. The Akt and p53 pathways are two important signaling pathways that are involved in G2/M transition by regulating CDK1 and CCNB1 [35,36]. As shown in Fig 8F, some *TMEM25*-associated DEGs are related to the p53 pathway. Thus, I assumed that the Akt and p53 pathways were affected by the *TMEM25* expression level in NPCs.

To understand the mechanism by which *TMEM25* promotes NPC proliferation, several pathways mentioned above were investigated. Western blotting showed that suppression of *TMEM25* in NPCs could repress EGF-induced activation of Akt (Fig. 11B,C), suggesting that *TMEM25* had considerable effects on Akt pathways. On the other hand, suppression of *TMEM25* in NPCs could alter phosphorylation status of p53 only faintly. Because previous reports showed that *TMEM25* interacted with the *N*-methyl-d-aspartate receptor *NR2B*, which is associated with the Creb pathway [22,37], I also checked whether *TMEM25* affected activation of Creb. However, as shown in Fig. 11B,C, knockdown of *TMEM25* did not affect the level of Creb phosphorylation.

To further prove that *TMEM25* regulated NPC proliferation through the Akt pathway, I performed rescue experiments by treatment with SC79, a specific Akt activator [38]. My results showed that after SC79 treatment, the phospho-Akt was significantly increased compared with that in untreated *TMEM25* knockdown NPCs (Fig. 11D,E). However, the phospho-p53 was not decreased (Fig. 11D,E), suggesting that *TMEM25* may not affect

the state of p53 activation through the Akt pathway. Akt activation could increase the cell proliferation ability of *TMEM25* knockdown NPCs back to normal levels (Fig. 12A,B). qPCR analysis showed the expression levels of *CDK1* and *CCNB1* were significantly increased after Akt activation, compared with the levels in *TMEM25* knockdown NPCs (Fig. 12C,D). Interestingly, the expression level of the human-specific gene, *ARHGAP11B*, was also recovered after treatment with SC79 (Fig. 12E,F). Taken together, these results suggest that *TMEM25* mainly regulates cell cycle progression via Akt activation and increased *CDK1*-*CCNB1* expression in NPCs.

Discussion

The summary of this study

In this study, I discovered that a conserved gene, *TMEM25*/*Tmem25*, could stimulate the proliferation of NPCs in mice. My experiments showed that overexpression of *TMEM25* in mice to mimic the human type of expression resulted in increased generation of BPs, particularly bRG, which facilitated the production of upper-layer neurons and supported cortical development (Fig. 5-7). Considering the knockdown data of *TMEM25* in human AF22 in which cell cycle was down-regulated (Fig. 2), *TMEM25* could also regulate the proliferation of human NPCs. As a possible mechanism of *TMEM25*-triggered NPC proliferation to enlarge the cortical structure reminiscent of human brain expansion, I also revealed that *TMEM25* is required for the regulation of *CDK1* and *CCNB1* expression via Akt signaling pathway. I will discuss the potential involvement of species-dependent alteration in gene expression regulation in diversifying the brain structure and function.

TMEM25 as an example of conserved genes for representing human-specific phenomena

Accumulating evidence has shown that human-specific genes play a key role in driving the expansion of the human Ncx [15-17,24,39]. During mammalian evolution, cortical expansion and folding have occurred gradually, and species-specific genes alone are insufficient to drive this process. In this context, fine tuning of the expressions of a number of conserved protein-coding genes may account for a part of these gradual steps in the accelerated cortical expansion and complex folding during the course of evolution. Among such genes with species-dependent differential expression, I propose that *TMEM25* has increased its expression to function in the derivation and the subsequent

proliferation of bRG through targeting human-specific pathways, as further discussed below.

Functions of *TMEM25* in the derivation and the subsequent amplification of bRGs

My experiments on overexpression of *TMEM25* in mouse embryos revealed that higher expression levels of *TMEM25* promote the proliferation of BPs in the SVZ (Fig. 5,6). In the SVZ, the number of bRG and bIPs determine cortical development. Previous studies showed that expanding bIPs only leads to an increase in brain size, while the expansion of bRG is closely linked to cortical folding [30,40]. This may explain why bRG are scarce in the mouse SVZ but more abundant and highly proliferative in humans [12]. I found that *TMEM25* upregulation increased the generation of Pax6+ or Sox2+ cells in the SVZ (Fig.5), whereas the increase in Tbr2+ cells was slight, which further proved that *TMEM25* upregulation promotes expansion of bRG. Therefore, human-biased expression of *TMEM25* in NPCs should be an important key for distinguishing humans from other animals via its contribution to the generation of higher ordered structure in brains through the abundant derivation of bRG.

It is widely accepted that the expansion of the mammalian neocortex during evolution was due to a high production of cortical neurons, brought about by an increase in the proliferation of NPCs followed by prolonged neurogenesis [41,42]. To mimic the low expression of *TMEM25* seen in mice, knockdown experiments of *TMEM25* were conducted in human NPCs. The results clearly showed that the downregulation of *TMEM25* significantly reduced the number of EdU+ NPCs and the expression level of *MKI67* (Fig.2), indicating that *TMEM25* plays an active role in regulating NPC proliferation. RNA-seq data showed that knockdown of *TMEM25* could significantly inhibit the expression of a variety of genes related to cell proliferation (Fig. 8B,C),

strongly suggesting that, during cortical development, the increase in the number of upper-layer neurons (fig.7) is due to an increase in the pool of NPCs promoted by *TMEM25*.

Intracellular mechanisms of human-specific amplification of NPCs triggered by *TMEM25*

TMEM25 facilitates phosphorylation of Akt to promote the expression of *CDK1/CCNB1*, which control the G2/M transition in the cell cycle. *CDK1/CCNB1* are responsible for maintaining human stem cells in a pluripotent state [43,44]. The up-regulation of *CCNB1* can keep RG in an undifferentiated state and promote upper-layer neurogenesis at the cost of consuming deep-layer identity [44]. This is similar to my finding that overexpression of *TMEM25* promotes the proliferation of bRG but not IPs to generate a large number of upper-layer neurons (Fig. 5-7). PI3k-Akt and p53 are two classical pathways involved in positive and negative regulation of NPC proliferation, respectively [45,46]. It is noteworthy that these two signaling pathways may serve as potential upstream regulators o*f CDK1* and *CCNB1* expressions [35,36]. Some studies proved that there is crosstalk between Akt and p53 through affecting MDM2 phosphorylation [47,48]. Recently, the evidence of *TMEM25* interacting specifically with epidermal growth factor receptor (EGFR) can be observed [49]. Furthermore, EGF binding to its receptor can activate several signaling intermediates, including Akt [50]. In response to EGF induction, the docking protein Gab1 binds to EGFR, thereby stimulating PI-3 kinase and Akt phosphorylation [51]. As shown in Fig. 11B, EGF stimulation to phosphorylate Akt was dependent on the presence of *TMEM25* in human AF22. Therefore, it is possible that *TMEM25* regulates Akt signaling through the interaction with EGFR. In this study, knockdown of *TMEM25* significantly inhibited Akt-signaling but slightly activated p53-

signaling to repress the expression of *CDK1* and *CCNB1*. I found the downregulation of *CDK1* and *CCNB1* after *TMEM25* knockdown, that was reversed by the treatment with a Akt signaling activator, SC79 (Fig. 12). The specific relationship between *TMEM25*-triggered phosphorylation of Akt and the transcriptional regulation of *CDK1* remains unknown. It's worth noting that both Akt and *CDK1* are involved in complex cellular pathways and their activities can be influenced by a multitude of factors. Therefore, pAkt could influence *CDK1* expression indirectly through a series of signaling cascades. Phosphorylation of p53 is also a candidate event that mediates the downregulation of *CDK1* expression as my analysis of downregulated genes by TMEM25 knockdown called p53 signaling pathway as a significantly overrepresented GO terms (Fig. 8F). However, western blotting data showed that *TMEM25* decreased phospho-p53 only faintly (Fig. 11B). Future study will delineate the exact signaling pathways stimulated by the species-dependent expression of *TMEM25* that have been established during human brain evolution.

Connection of *TMEM25*-triggered pathway with the network of human-specific genes

Interestingly, upon knocking down *TMEM25*, I observed a significant decrease in the expression of *ARHGAP11B* (Fig. 8C). It has been reported that *ARHGAP11B* facilitates the proliferation of BPs by inhibition of mPTP which allows mitochondria to acquire a higher Ca^{2+} concentration to increase the progression of the TCA cycle [39]. As shown in Fig. 9, overexpression of *ARHGAP11B* rescued the cell proliferation which was inhibited by knockdown of *TMEM25*. It is possible that *TMEM25* serves as a crucial upstream regulator of *ARHGAP11B* to modulate mitochondrial function affecting cortical

development. Interestingly, Akt has been known to phosphorylate MICU1 to increase mitochondrial Ca^{2+} at resting conditions [52]. Although I still do not know how *ARHGAP11B* is induced by the phospho-Akt, *ARHGAP11B* and Akt signaling may cooperate at mitochondria to finely tune the NPC proliferation in a human-specific manner. On the other hand, other human-specific genes such as *TMEM14B* and *NOTCH2NL* were not affected by *TMEM25* knockdown. I therefore suppose that there should be mechanisms involving human-specific genes and/or conserved genes with species-dependent expression other than the *TMEM25-ARHGAP11B* network, that would add new layers of organizing brain functions in humans.

Because *ARHGAP11B* is a human specific gene, I think it is possible that there are some differences in the effects of *TMEM25* between mouse and human NPCs. Normally, TMEM25-Akt-CDK1 constitutes a molecular axis that is commonly used in human and mouse NPCs, whereas TMEM25-Akt-ARHGAP11B pathway can be an additional molecular axis to support increased proliferation in the developing cortex in humans. In fact, I found only the proliferation of bRG, but not that of bIPs after *TMEM25* overexpression in mice (Fig. 5,6), whereas previous *in vivo* experiments have shown that *ARHGAP11B* can promote expansion of bIPs in mice [24]. Clearly, more evidence is needed to further support this hypothesis.

The potential involvement of human-specific non-coding RNAs to achieve human-biased expression of conserved genes

The previous research demonstrated that the presence of high GC content in the promoter tends to generate divergent lncRNAs upstream of genes in a head-to-head manner (referred to as pancRNAs) [27,53,54]. pancRNAs have the ability to participate in various

biological processes through specifically up-regulating the partner mRNAs [53]. Compared with protein coding genes, pancRNAs exhibit greater species specificity, implying that the acquisition of human-specific pancRNAs may lead to a surge in the expression levels of certain conserved genes during evolution. My findings indicated that expression level of *TMEM25* was significantly higher in humans than in mice, and that *pancTMEM25* is exclusively present in the human genome (Fig. 1), hinting that evolutionary acquisition of *pancTMEM25* was a key to accomplishing the human-biased expression of highly conserved genes that functions in maintaining prolonged proliferation of bRG. Further research would fully elucidate the mechanism by which *pancTMEM25* was acquired in modifying the genomic structure of *TMEM25* to potentially regulate gene expression.

In conclusion, my study provides evidence that the evolutionarily differentiated genomic structure of *TMEM25* promotes fine tuning of RNA expression from this locus to realize human-specific usage of this conserved gene for accelerating proliferation of NPCs, especially bRG. *TMEM* family genes have been expanded in two ways, i.e., by generating a human-specific homolog (*TMEM14B*) and by differentiating the expression mode by changing promoter usage of a conserved gene (*TMEM25*). Since other candidates that are potentially involved in the human-specific features, such as *TMEM51* (Fig. 1D), have also been found, my study would be a landmark for understanding the mechanisms of evolutionary brain expansion by the coordination of both human-specific and species-dependently expressed conserved *TMEM* family genes.

Acknowledgements

I am very grateful to my supervisor, Professor Imamura, who always helps me and supports me no matter in life or research, so that I have made progress in academics and Japanese learning. I would also like to thank Tomonori Kameda and all members in Laboratory of Molecular and Cellular Physiology. Their presence makes my study abroad life more colorful, and I am also very happy to become good friends with them. Finally, I want to thank my family for their support for my study abroad.

References

1 Florio, M. and Huttner, W.B. (2014). Neural progenitors, neurogenesis and the evolution of the neocortex. Development 141, 2182-2194.

2 Ju, X.C., Hou, Q.Q., Sheng, A.L., Wu, K.Y., Zhou, Y., Jin, Y., Wen, T., Yang, Z., Wang, X and Luo, Z.G. (2016). The hominoid-specific gene TBC1D3 promotes generation of basal neural progenitors and induces cortical folding in mice. Elife 5, 25.

3 Rakic, P. (1995). A small step for the cell, a giant leap for mankind- a hypothesis of neocortical expansion during evolution. Trends in Neurosciences 18, 383-388.

4 Geschwind, D.H. and Rakic, P. (2013). Cortical Evolution: Judge the Brain by Its Cover. Neuron 80, 633-647.

5 Molnar, Z., Metin, C., Stoykova, A., Tarabykin, V., J. Price, D., Francis, F., Meyer, G., Dehay, C. and Kennedy, H. (2006). Comparative aspects of cerebral cortical development. European Journal of Neuroscience 23, 921-934.

6 Sousa, A.M.M., Meyer, K.A., Santpere, G., Gulden, F.O. and Sestan, N. (2017). Evolution of the Human Nervous System Function, Structure, and Development. Cell 170, 226-247.

7 Namba, T. and Huttner, W.B. (2017). Neural progenitor cells and their role in the development and evolutionary expansion of the neocortex. Wiley Interdisciplinary Reviews-Developmental Biology 6, 16.

8 Xing, L., Kalebic, N., Namba, T., Vaid, S., Wimberger, P. and Huttner, W.B. (2020). Serotonin Receptor 2A Activation Promotes Evolutionarily Relevant Basal Progenitor Proliferation in the Developing Neocortex. Neuron 108, 24.

9 Haubensak, W., Attardo, A., Denk, W. and Huttner, W.B. (2004). Neurons arise in the basal neuroepithelium of the early mammalian telencephalon: A major site of neurogenesis. Proceedings of the National Academy of Sciences of the United States of America 101, 3196-3201.

10 Miyata, T., Kawaguchi, A., Saito, K., Kawano, M., Muto, T. and Ogawa, M. (2004). Asymmetric production of surface-dividing and non-surface-dividing cortical progenitor cells. Development 131, 3133-3145.

11 Noctor, S.C., Martinez-Cerdeno, V., Ivic, L. and Kriegstein, A.R. (2004). Cortical neurons arise in symmetric and asymmetric division zones and migrate through specific phases. Nature Neuroscience 7, 136-144.

12 Kalebic, N., Gilardi, C., Stepien, B., Wilsch-brauninger, M., Long, K.R., Namba, T., Florio, M., Langen, B., Lombardot, B., Shevchenko, A., Kilimann, M.W., Kawasaki, H., Wimberger, P. and Huttner, W.B. (2019). Neocortical Expansion Due to Increased Proliferation of Basal Progenitors Is Linked to Changes in Their Morphology. Cell Stem Cell 24, 535-550.

13 Dehay, C., Kennedy, H. and Kosik, K.S. (2015). The Outer Subventricular Zone and Primate-Specific Cortical Complexification. Neuron 85, 683-694.

14 Borrell, V. and Reillo, I. (2012). Emerging roles of neural stem cells in cerebral cortex development and evolution. Developmental Neurobiology 72, 955-971.

15 Liu, J., Liu, W., Yang, L., Wu, Q., Zhang, H., Fang, A., Li, L., Xu, X., Sun, L., Zhang, J., Tang, F. and Wang, X. (2017). The Primate-Specific Gene TMEM14B Marks Outer Radial Glia Cells and Promotes Cortical Expansion and Folding. Cell Stem Cell 21, 635-649.

16 Suzuki, I.K., Gacquer, D., Heurck, R.V., Kumar, D., Wojno, M., Bilheu, A., Herpoel, A., Lambert, N., Cheron, J., Polleux, F., Detours, V. and Vanderhaeghen, P. (2018). Human-Specific NOTCH2NL Genes Expand Cortical Neurogenesis through Delta/Notch Regulation. Cell 173, 1370-1384.

17 Hou, Q.Q., Xiao, Q., Sun, X.Y., Ju, X.C. and Luo, Z.G. (2021). TBC1D3 promotes neural progenitor proliferation by suppressing the histone methyltransferase G9a. Science Advances 7, 13.

18 Dodeller, F., Gottar, M., Huesken, D., Iourgenko, V. and Cenni, B. (2008). The lysosomal transmembrane protein 9B regulates the activity of inflammatory signaling pathways. Journal of Biological Chemistry 283, 21487-21494.

19 Schmit, K. and Michiels, C. (2018). TMEM Proteins in Cancer: A Review. Frontiers in

Pharmacology 9, 13.
20 Cheng, Z.P., Guo, J., Chen, L., Luo, N., Yang, W.H. and Qu, X.Y. (2015). Overexpression of TMEM158 contributes to ovarian carcinogenesis. Journal of Experimental & Clinical Cancer Research 34, 9.
21 Hrasovec, S., Hauptman, N., Glavac, D., Jelenc, F. and Ravnik-Glavac, M. (2013). TMEM25 is a candidate biomarker methylated and down-regulated in colorectal cancer. Disease Markers 34, 93-104.
22 Zhang, H.Q., Tian, X., Lu, X., Xu, D.M., Guo, Y., Dong, Z.F., Li, Y., Ma, Y.L., Chen, C.Z., Yang, Y., Yang, M., Yang, Y., Liu, F., Zhou, R.J., He, M.Q., Xiao, F. and Wang, X.F. (2019). TMEM25 modulates neuronal excitability and NMDA receptor subunit NR2B degradation. Journal of Clinical Investigation 129, 3864-3876.
23 Barkovich, A.J., Dobyns, W.B. and Guerrini, R. (2015). Malformations of Cortical Development and Epilepsy. Cold Spring Harbor Perspectives in Medicine 5, 23.
24 Florio, M., Albert, M., Taverna, E., Namba, T., Brandl. H., Lewitus, E., Haffner, C., Sykes, A., Wong, F.K., Peters, J., Guhr, E., Klemroth, S., Prufer, K., Kelso, J., Naumann, R., Nusslein, I., Dahl, A., Lachmann, R., Paabo, S. and Huttner, W.B. (2015). Human-specific gene ARHGAP11B promotes basal progenitor amplification and neocortex expansion. Science 347, 1465-1470.
25 Hamazaki, N., Uesaka, M., Nakashima, K., Agata, K. and Imamura, T. (2015). Gene activation-associated long noncoding RNAs function in mouse preimplantation development. Development 142, 910-920.
26 Yamamoto, N., Agata, K., Nakashima, K. and Imamura, T. (2016). Bidirectional promoters link cAMP signaling with irreversible differentiation through promoter-associated non-coding RNA (pancRNA) expression in PC12 cells. Nucleic Acids Research 44, 5105-5122.
27 Uesaka, M., Agata, K., Oishi, T., Nakashima, K. and Imamura, T. (2017). Evolutionary acquisition of promoterassociated non-coding RNA (pancRNA) repertoires diversifies species-dependent gene activation mechanisms in mammals. Bmc Genomics 18, 13.
28 Brattas, P.L., Jonsson, M.E., Fasching, L., Wahlestedt, J.N., Shahsavani, M., Falk, A., Jern, P., Parmar, M. and Jakobsson, J. (2017). TRIM28 Controls a Gene Regulatory Network Based on Endogenous Retroviruses in Human Neural Progenitor Cells. Cell Reports 18, 1-11.
29 Fietz, S.A., Lachmann, R., Brandl, H., Kircher, M., Samusik, N., Schroder, R., Lakshmanaperumal, N., Henry, I., Vogt, J., Riehn, A., Distler, W., Nitsch, R., Enard, W., Paabo, S. and Huttner, W.B. (2012). Transcriptomes of germinal zones of human and mouse fetal neocortex suggest a role of extracellular matrix in progenitor self-renewal. Proceedings of the National Academy of Sciences of the United States of America 109, 11836-11841.
30 Nonaka-Kinoshita, M., Reillo, I., Artegiani, B., Martinez-Martinez, M.A., Nelson, M., Borrell, V. and Calegari, F. (2013). Regulation of cerebral cortex size and folding by expansion of basal progenitors. Embo Journal 32, 1817-1828.
31 Lui, J.H., Hansen, D.V. and Kriegstein, A.R. (2011). Development and Evolution of the Human Neocortex. Cell 146, 18-36.
32 Kerimoglu, C., Pham, L., Tonchev, A.B., Sakib, M.S., Xie, Y., Sokpor, G., Ulmke, P.A., Kaurani, L., Abbas, E., Nguyen, H., Rosenbusch, J., Michurina, A., Capece, V., Angelova, M., Maricic, N., Brand-Saberi, B., Esgleas, M., Albert, M., Minkov, R., Kovachev, E., Teichmann, U., Seong, R.H., Huttner, W.B., Nguyen, H.P., Stoykova, A., Staiger, J.F., Fischer, A. and Tuoc, T. (2021). H3 acetylation selectively promotes basal progenitor proliferation and neocortex expansion. Science Advances 7, 17.
33 Sancar, A., Lindsey-Boltz, L.A., Unsal-Kacmaz, K. and Linn, S. (2004). Molecular mechanisms of mammalian DNA repair and the DNA damage checkpoints. Annual Review of Biochemistry 73, 39-85.
34 Kastan, M.B. and Bartek, J. (2004). Cell-cycle checkpoints and cancer. Nature 432, 316-323.
35 Taylor, W.R. and Stark, G.R. (2001). Regulation of the G2/M transition by p53. Oncogene 20, 1803-1815.
36 Lin, C.C., He, Y., Feng, Q., Xu, K., Chen, Z., Tao, B.L., Li, X.M., Xia, Z.Z., Jiang, H. and Cai,

K.Y. (2021). Self-renewal or quiescence? Orchestrating the fate of mesenchymal stem cells by matrix viscoelasticity via PI3K/Akt-CDK1 pathway. Biomaterials 279, 15.

37 Ramirez, M. and Lamas, M. (2009). NMDA receptor mediates proliferation and CREB phosphorylation in postnatal Muller glia-derived retinal progenitors. Molecular Vision 15, 713-721.

38 Jo, H., Mondal, S., Tan, D., Nagata, E., Takizawa, S., Sharma, A.K., Hou, Q., Shanmugasundaram, K., Prasad, A., Tung, J.K., Tejeda, A.O., Man, H., Rigby, A.C. and Luo, H.R. (2012). Small molecule-induced cytosolic activation of protein kinase Akt rescues ischemia-elicited neuronal death. Proceedings of the National Academy of Sciences of the United States of America 109, 10581-10586.

39 Namba, T., Doczi, J., Pinson, A., Xing, L., Kalebic, N., Wilsch-Brauninger, M., Long, K.R., Vaid, S., Lauer, J., Bogdanova, A., Borgonovo, B., Shevchenko, A., keller, P., Drechsel, D., Kurzchalia, T., Wimberger, P., Chinopoulos, C. and Huttner, W.B. (2020). Human-Specific ARHGAP11B Acts in Mitochondria to Expand Neocortical Progenitors by Glutaminolysis. Neuron 105, 867-881.

40 Betizeau, M., Cortay, V., Patti, D., Pfister, S., Gautier, E., Bellemin-Menard, A., Afanassieff, M., Huissoud, C., Douglas, R.J., Kennedy, H. and Dehay, C. (2013). Precursor Diversity and Complexity of Lineage Relationships in the Outer Subventricular Zone of the Primate. Neuron 80, 442-457.

41 Llinares-Benadero, C. and Borrell, V. (2019). Deconstructing cortical folding: genetic, cellular and mechanical determinants. Nature Reviews Neuroscience 20, 161-176.

42 Zilles, K., Palomero-Gallagher, N. and Amunts, K. (2013). Development of cortical folding during evolution and ontogeny. Trends in Neurosciences 36, 275-284.

43 Gonzales, K.A.U. et al. (2015). Deterministic Restriction on Pluripotent State Dissolution by Cell-Cycle Pathways. Cell 162, 564-579.

44 Hagey, D.W., Topcic, D., Kee, N., Reynaud, F., Bergsland, M., Perlmann, T. and Muhr, J. (2020). CYCLIN-B1/2 and-D1 act in opposition to coordinate cortical progenitor self-renewal and lineage commitment. Nature Communications 11, 16.

45 Zhou, Z.Y., Dun, L.L., Wei, B.X., Gan, Y.Y., Liao, Z.L., Lin, X.M., Lu, J.L., Liu, G.C., Xu, H., Lu, C.J. and An, H.W. (2020). Musk Ketone Induces Neural Stem Cell Proliferation and Differentiation in Cerebral Ischemia via Activation of the PI3K/Akt Signaling Pathway. Neuroscience 435, 1-9.

46 Meletis, K., Wirta, V., Hede, S.M., Nister, M., Lundeberg, J. and Frisen, J. (2006). P53 suppresses the self-renewal of adult neural stem cells. Development 133, 363-369.

47 Gottlieb, T.M., Leal, J.F.M., Seger, R., Taya, Y. and Oren, M. (2002). Cross-talk between Akt, p53 and Mdm2: possible implications for the regulation of apoptosis. Oncogene 21, 1299-1303.

48 Liu, T., Ren, D., Zhu, X., Yin, Z., Jin, G., Zhao, Z., Robinson, D., Li, X., Wong, K., Cui, K., Zhao, H. and Wong, S.T.C. (2013). Transcriptional signaling pathways inversely regulated in Alzheimer's disease and glioblastoma multiform. Scientific Reports 3, 10.

49 Bi, J., Wu, Z., Zhang, X., Zeng, T., Dai, W., Qiu, N., Xu, M., Qiao, Y., Ke, L., Zhao, J., Cao, X., Lin, Q., Chen, X.L., Xie, L., Ouyang, Z., Guo, J., Zheng, L., Ma, C., Guo, S., Chen, K., Mo, W., Fu, G., Zhao, T.J. and Wang, H.R. (2023). TMEM25 inhibits monomeric EGFR-mediated STAT3 activation in basal state to suppress triple-negative breast cancer progression. Nature Communications 14, 15.

50 Garay, C., Judge, G., Lucarelli, S., Bautista, S., Pandey, R., Singh, T. and Antonescu, C.N. (2015). Epidermal growth factor-stimulated Akt phosphorylation requires clathrin or ErbB2 but not receptor endocytosis. Molecular Biology of the Cell 26, 3504-3519.

51 Mattoon, D.R., Lamothe, B., Lax, I. and Schlessinger, J. (2004). The docking protein Gab1 is the primary mediator of EGF-stimulated activation of the PI-3K/Akt cell survival pathway. Bmc Biology 2, 12.

52 Marchi, S., Corricelli, M., Branchini, A., Vitto, V.A.M., Missiroli, S., Morciano, G., Perrone, M., Ferrarese, M., Giorgi, C., Pinotti, M., Galluzzi, L., Kroemer, G. and Pinton, P. (2019). Akt-

mediated phosphorylation of MICU1 regulates mitochondrial Ca2+ levels and tumor growth. Embo Journal 38, 20.

53 An, B.Y., Kameda, T. and Imamura, T. (2021) The evolutionary acquisition and mode of functions of promoter-associated non-coding RNAs (pancRNAs) for mammalian development. Essays in Biochemistry EBC20200143.

54 Uesaka, M., Nishimura, O., Go, Y., Nakashima, K., Agata, K. and Imamura, T. (2014). Bidirectional promoters are the major source of gene activation-associated non-coding RNAs in mammals. Bmc Genomics 15, 14.

55 Nakashima, H., Tsujimura, K., Irie, K., Imamura, T., Trujillo, C.A., Ishizu, M., Uesaka, M., Pan, M., Noguchi, H., Okada, K., Aoyagi, K., Andoh-Noda, T., Okano, H., Muotri, A.R. and Nakashima, K. (2021). MeCP2 controls neural stem cell fate specification through miR-199a-mediated inhibition of BMP-Smad signaling. Cell Reports 35, 19.

56 Lois, C., Hong, E.J., Pease, S., Brown, E.J. and Baltimore, D. (2002). Germline transmission and tissue-specific expression of transgenes delivered by lentiviral vectors. Science 295, 868-872.

57 Zhou, Z.L. , Hong, E.J., Cohen, S., Zhao, W.N., Ho, H.Y.H., Schmidt, L., Chen, W.G., Lin, Y., Savner, E., Griffith, E.C., Hu, L., Steen, J.A.J., Weitz, C.J. and Greenberg, M.E. (2006). Brain-specific phosphorylation of MeCP2 regulates activity-dependent Bdnf transcription, dendritic growth, and spine maturation. Neuron 52, 255-269.

58 Dobin, A., Davis, C.A., Schlesinger, F., Drenkow, J., Zaleski, C., Jha, S., Batut, P., Chaisson, M. and Gingeras, T.R. (2013). STAR: ultrafast universal RNA-seq aligner. Bioinformatics 29, 15-21.

59 Quinlan, A.R. and Hall, I.M. (2010). BEDTools: a flexible suite of utilities for comparing genomic features. Bioinformatics 26, 841-842.

Figures

Figure 1

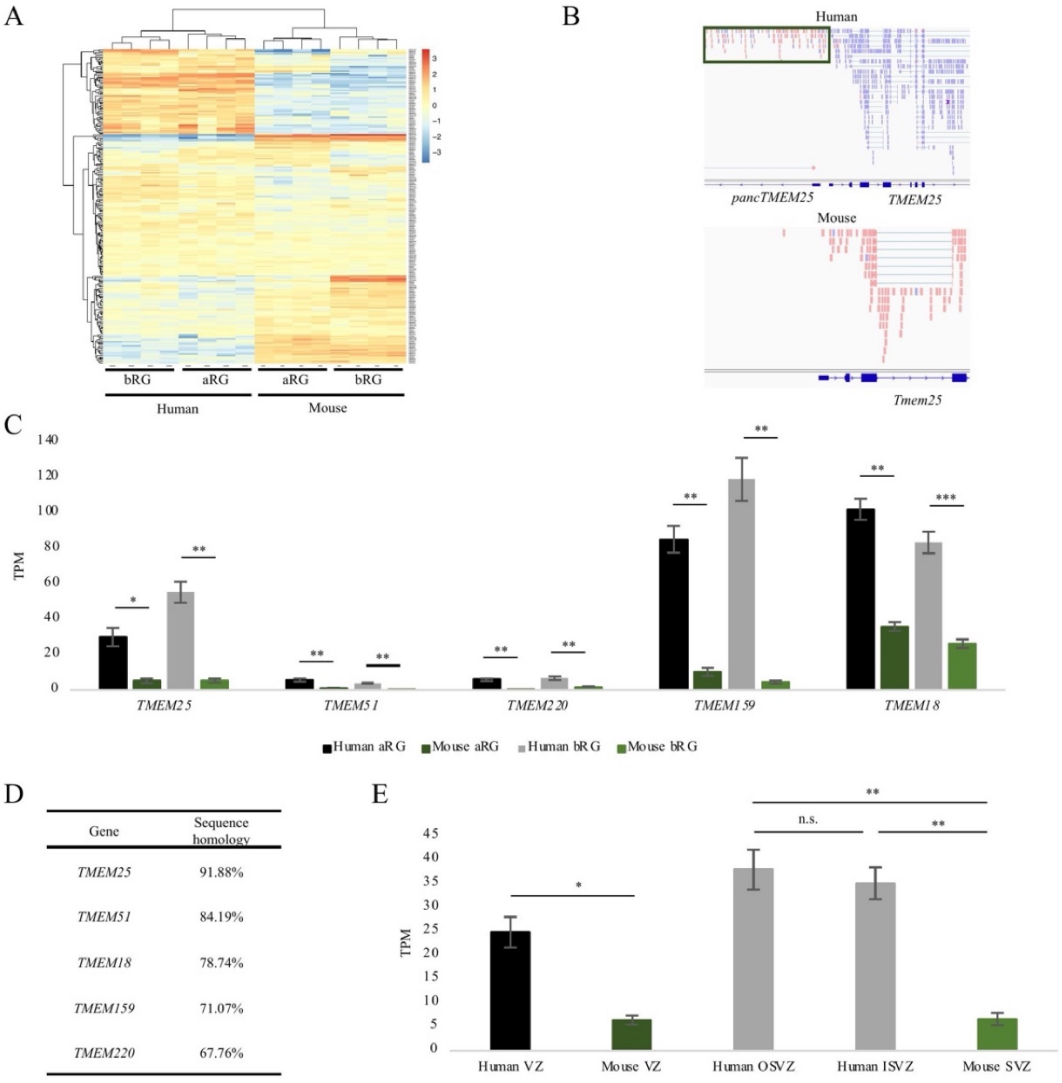

Gene	Sequence homology
TMEM25	91.88%
TMEM51	84.19%
TMEM18	78.74%
TMEM159	71.07%
TMEM220	67.76%

Figure 1. *TMEM25* is highly expressed in human neocortex compared to mouse neocortex among the TMEM family

(A) Heatmap of DEGs in *TMEM* family between aRG and bRG of humans and of mice. DEGs between aRG and bRG were extracted for humans and mice by calculating the log2 value relative to average TPM, and DEGs were represented by color. (B) Diagram of the *pancTMEM25* and *TMEM25* gene locus in human and mouse. (C) Expression levels of *TMEM25*, *TMEM51*, *TMEM220*, *TMEM159* and *TMEM18* in aRG and bRG of humans and mice. (D) Sequence homology of *TMEM25*, *TMEM51*, *TMEM220*, *TMEM159* and *TMEM18* between human and mouse. (E) Expression levels of *TMEM25* in VZ and SVZ of humans and mice. OSVZ: outer SVZ; ISVZ: inner SVZ. N = 3; *$p < 0.05$, **$p < 0.01$, ***$p < 0.001$.

Figure 2

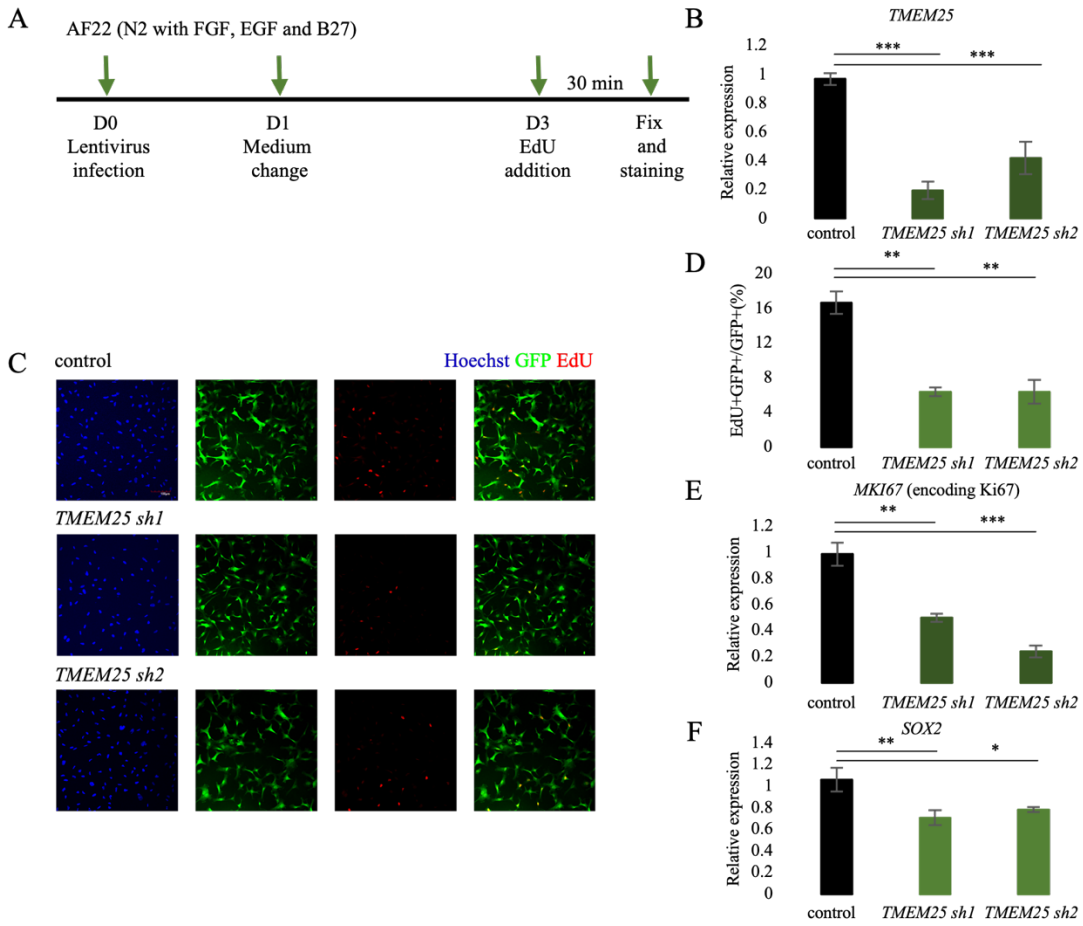
A
AF22 (N2 with FGF, EGF and B27)
30 min
D0
Lentivirus
infection
D1
Medium
change
D3
EdU
addition
Fix
and
staining
B
TMEM25
Relative expression
control
TMEM25 sh1
TMEM25 sh2
C
control
Hoechst GFP EdU
TMEM25 sh1
TMEM25 sh2
D
EdU+GFP+/GFP+(%)
E
MKI67 (encoding Ki67)
F
SOX2

Figure 2. *TMEM25* is necessary for NPC proliferation

(A) Experimental scheme to detect the effect of knockdown of *TMEM25* on the proliferation of AF22, and cells were harvested at the indicated time. (B) Quantification of the mRNA level of *TMEM25* after knockdown of *TMEM25*. (C) Representative images of the NPCs stained for GFP (green) and EdU (red) in control and knockdown of *TMEM25*. Nuclei were stained with Hoechst (blue). (D) Quantification of EdU+GFP+ to GFP+ cells in (C). (E, F) Quantification of the mRNA level of *MKI67* and *SOX2* after knockdown of *TMEM25*. N = 3; Scale bar = 100 um; *p < 0.05, **p < 0.01, ***p < 0.001, n.s.: not significant.

Figure 3

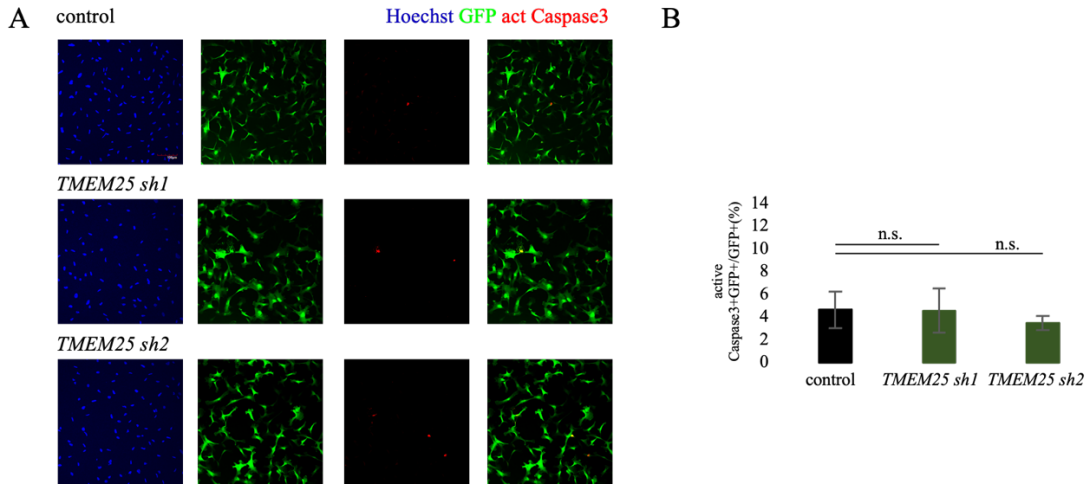
A
control
Hoechst GFP act Caspase3
TMEM25 sh1
TMEM25 sh2
B
active Caspase3+GFP+/GFP+(%)
14
12
10
8
6
4
2
0
n.s.
n.s.
control
TMEM25 sh1
TMEM25 sh2

Figure 3. *TMEM25* cannot affect NPC survival

(A) Representative images of the NPCs stained for GFP (green) and active Caspase3 (red) in control and knockdown of *TMEM25*. Nuclei were stained with Hoechst (blue). (B) Quantification of active Caspase3+GFP+ to GFP+ cells in (A). N = 3; Scale bar = 100 um; *p < 0.05, **p < 0.01, ***p < 0.001, n.s.: not significant.

Figure 4

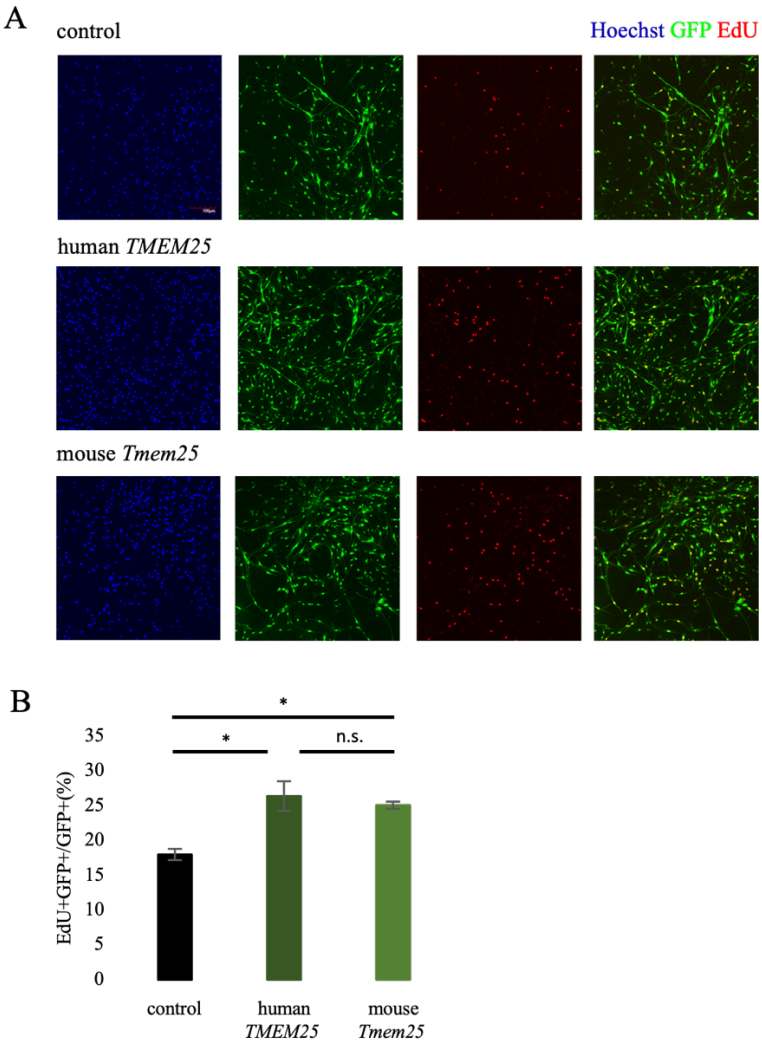
A
control
Hoechst GFP EdU
human TMEM25
mouse Tmem25
B
*
*
n.s.
35
30
25
20
15
10
5
0
EdU+GFP+/GFP+(%)
control
human TMEM25
mouse Tmem25

Figure 4. Expression level of *TMEM25* decides neurogenesis difference between human and mouse

(A) Representative images of the NPCs stained for GFP (green) and EdU (red) in control, overexpression of human *TMEM25* and overexpression of mouse *Tmem25*. Nuclei were stained with Hoechst (blue). (B) Quantification of EdU+GFP+ relative to GFP+ cells in (A). N = 3; Scale bar = 100um; *p < 0.05, n.s.: not significant.

Figure 5

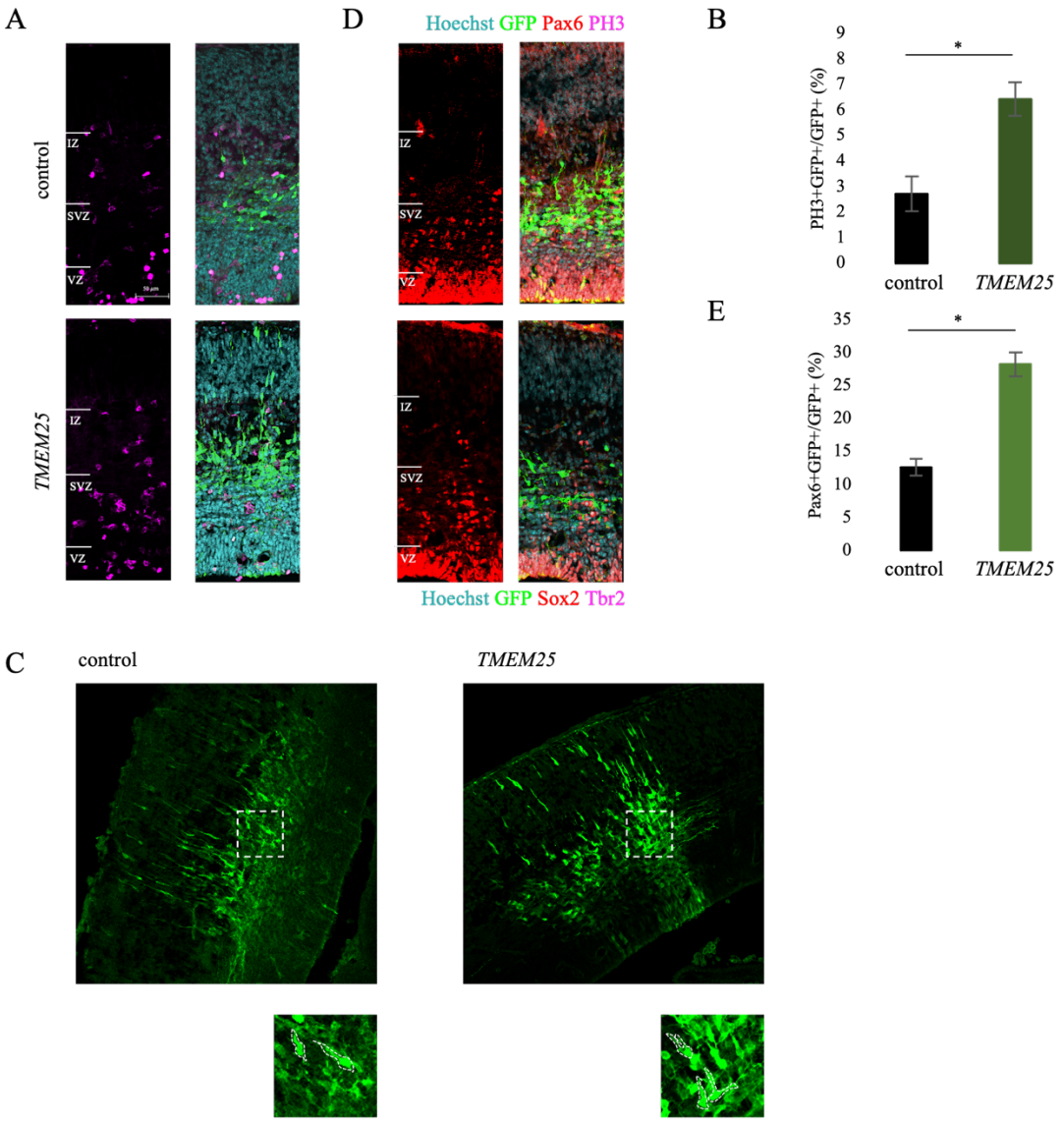
A
control
TMEM25
IZ
SVZ
VZ
D
Hoechst GFP Pax6 PH3
Hoechst GFP Sox2 Tbr2
B
PH3+GFP+/GFP+ (%)
control
TMEM25
E
Pax6+GFP+/GFP+ (%)
control
TMEM25
C
control
TMEM25

Figure 5. Human *TMEM25* expression promotes cortical development through increasing basal radial glia

(A) Representative images of the cortical slices stained for GFP (green) and PH3 (magenta) in control and *TMEM25*-overexpressing developing mice at E15.5. Nuclei were stained with Hoechst (blue). (B) Quantification of the percentage of PH3+ cells among GFP+ cells. (C) There are some cells with bRG morphology in electroporated cells. (D) Representative images of the cortical slices stained for GFP (green), Pax6 (red) in control and *TMEM25*-overexpressing E15.5 developing mice. Nuclei were stained with Hoechst (blue). (E) Quantification of the percentage of Pax6+ cells among GFP+ cells. N = 8; Scale bar = 50 um; *$p < 0.05$, n.s.: not significant.

Figure 6

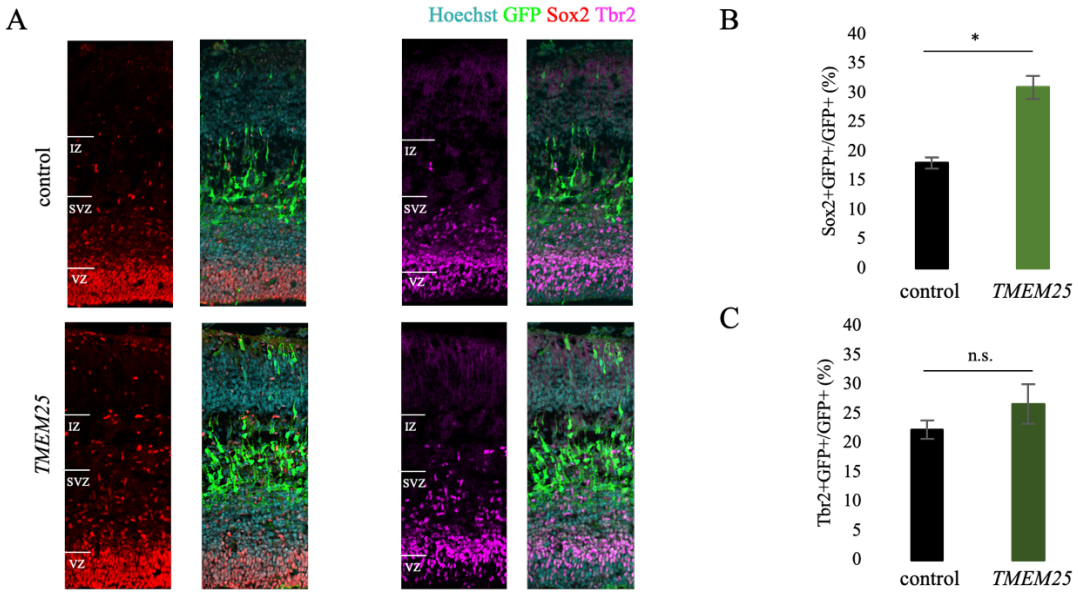
A
Hoechst GFP Sox2 Tbr2
control
TMEM25
IZ
SVZ
VZ
B
Sox2+GFP+/GFP+ (%)
40
35
30
25
20
15
10
5
0
*
control
TMEM25
C
Tbr2+GFP+/GFP+ (%)
40
35
30
25
20
15
10
5
0
n.s.
control
TMEM25

Figure 6. Human *TMEM25* expression does not increase in increased basal intermediate progenitors

(A) Representative images of the cortical slices stained for GFP (green), Sox2 (red) and Tbr2 (magenta) in control, and *TMEM25*-overexpressing E15.5 developing mice. Nuclei were stained with Hoechst (blue). (B) Quantification of the percentage of Sox2+ cells among GFP+ cells in SVZ. (C) Quantification of the percentage of Tbr2+ cells among GFP+ cells in SVZ. N = 8; Scale bar = 50 um; *$p < 0.05$, **$p < 0.01$, n.s.: not significant.

Figure 7

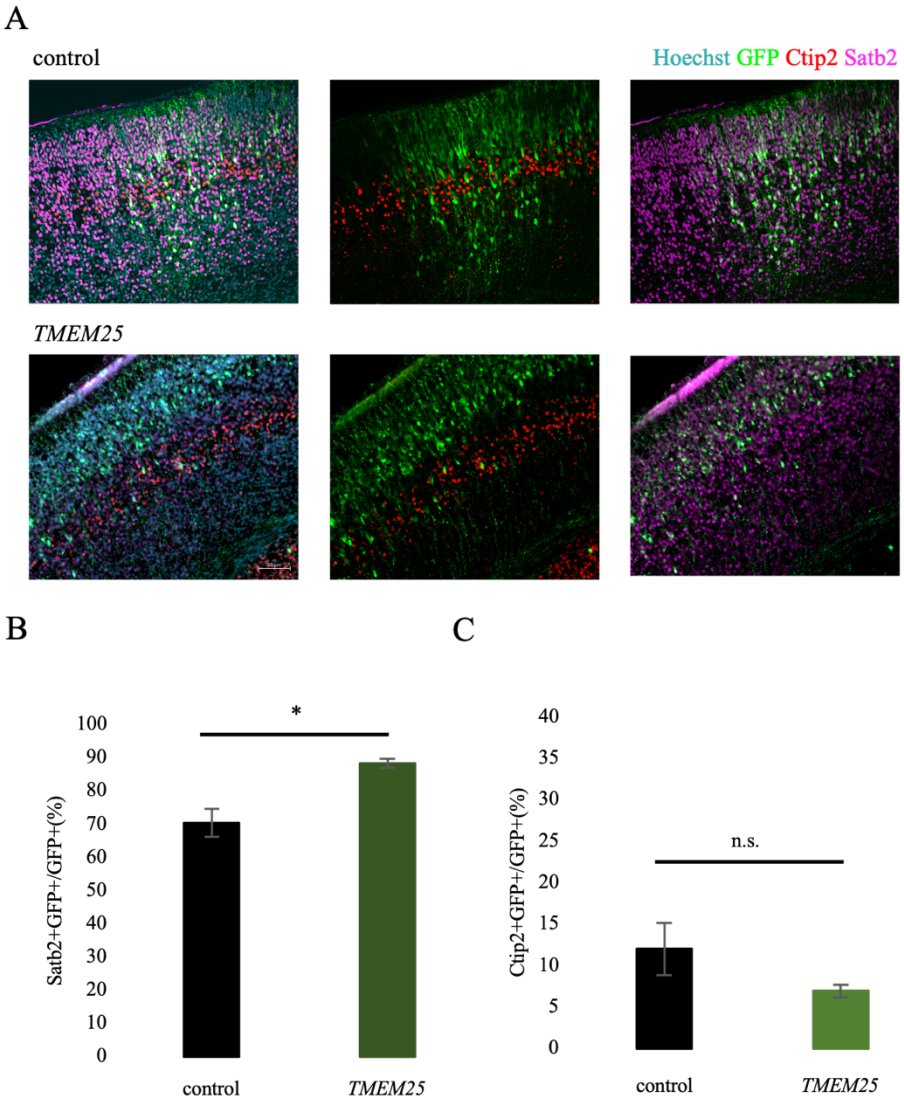
A
control
Hoechst GFP Ctip2 Satb2
TMEM25
B
C
Satb2+GFP+/GFP+(%)
100
90
80
70
60
50
40
30
20
10
0
*
control
TMEM25
Ctip2+GFP+/GFP+(%)
40
35
30
25
20
15
10
5
0
n.s.
control
TMEM25

Figure 7. Human *TMEM25* expression promotes cortical development through increasing upper-layer neurons

(A) Representative images of the cortical slices stained for GFP (green), Ctip2 (red), and Satb2 (magenta) in control and *TMEM25*-overexpressing E18.5 developing mice. Nuclei were stained with Hoechst (blue). (B) Quantification of the percentage of Satb2+ cells among GFP+ cells. (C) Quantification of the percentage of Ctip2+ cells among GFP+ cells. N = 7; Scale bar = 50 um; Scale bar = 50 um; **p < 0.01, n.s.: not significant.

Figure 8

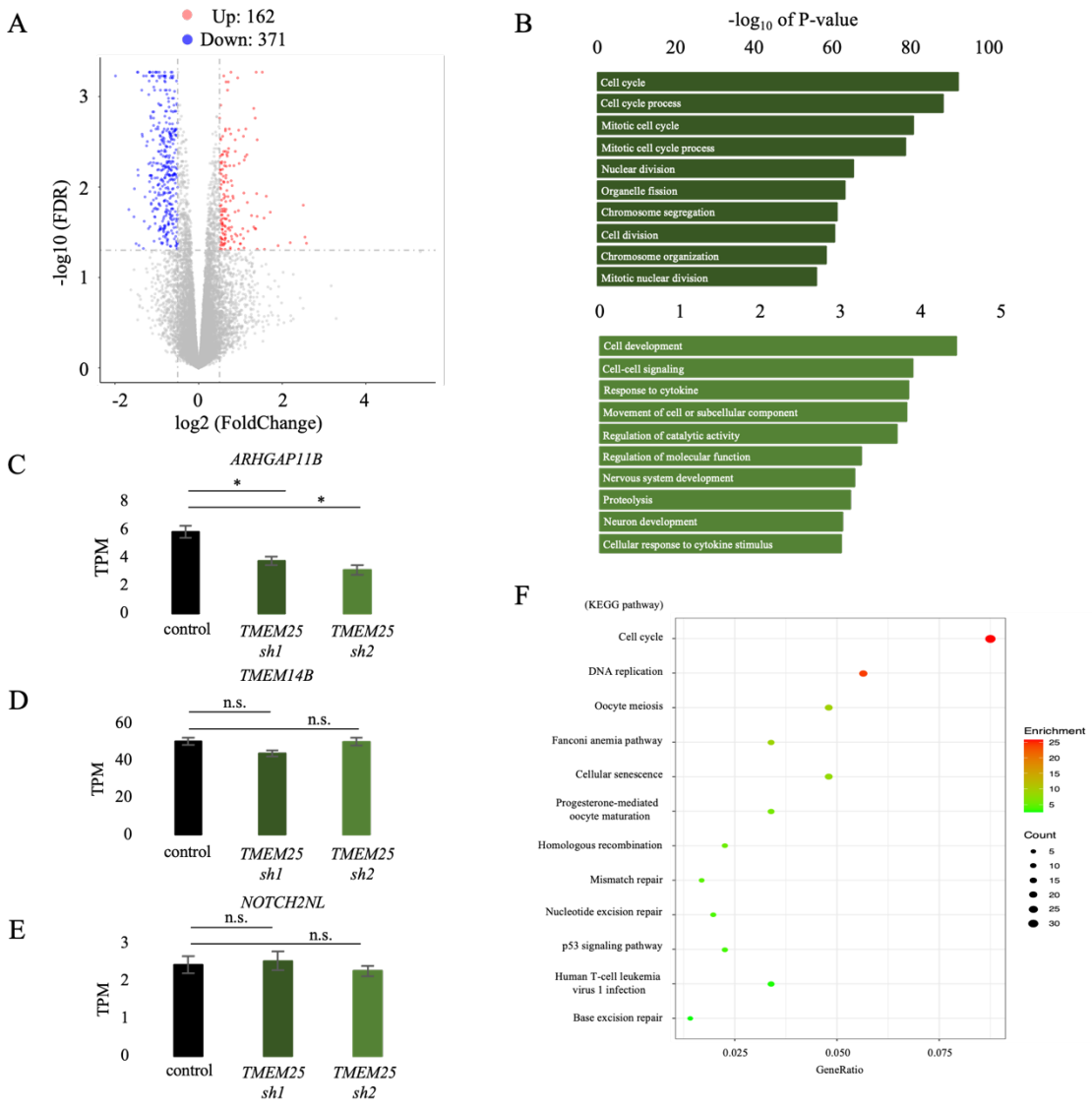
A
Up: 162
Down: 371
-log10 (FDR)
log2 (FoldChange)
B
-log10 of P-value
Cell cycle
Cell cycle process
Mitotic cell cycle
Mitotic cell cycle process
Nuclear division
Organelle fission
Chromosome segregation
Cell division
Chromosome organization
Mitotic nuclear division
Cell development
Cell-cell signaling
Response to cytokine
Movement of cell or subcellular component
Regulation of catalytic activity
Regulation of molecular function
Nervous system development
Proteolysis
Neuron development
Cellular response to cytokine stimulus
C
ARHGAP11B
TPM
control
TMEM25 sh1
TMEM25 sh2
D
TMEM14B
n.s.
E
NOTCH2NL
F
(KEGG pathway)
Cell cycle
DNA replication
Oocyte meiosis
Fanconi anemia pathway
Cellular senescence
Progesterone-mediated oocyte maturation
Homologous recombination
Mismatch repair
Nucleotide excision repair
p53 signaling pathway
Human T-cell leukemia virus 1 infection
Base excision repair
GeneRatio
Enrichment
Count

Figure 8. *TEME25* knockdown results in dysfunctional expression of genes associated with NPC physiological processes

(A) Volcano plot for the merged clusters obtained by RNA-seq analysis of control and *TMEM25*-knockdown NPCs. FDR < 0.05; log2 fold change ≥ 0.5. (B) GO-enrichment analysis of DEGs in *TMEM25*-knockdown NPCs. The top 10 enriched GO-terms for down-regulated (upper) and for up-regulated (lower) DEGs are indicated. (C, D and E) Expression levels of *ARHGAP11B*, *TMEM14B* and *NOTCH2NL* in control and *TMEM25*-knockdown NPCs. (F) KEGG pathway analysis of down-regulated DEGs in *TMEM25*-knockdown NPCs. n = 3; *p < 0.05, **p < 0.01.

Figure 9

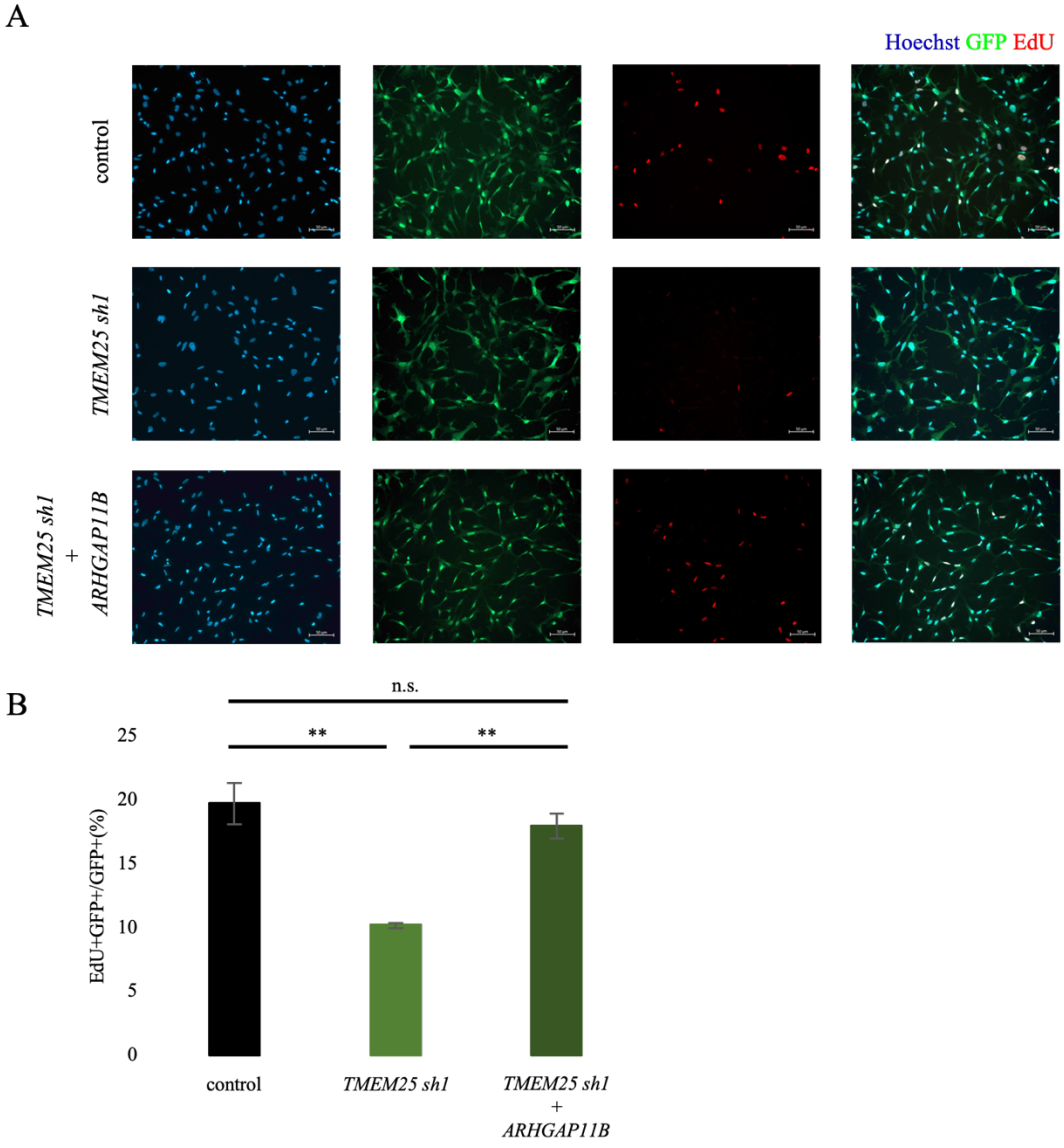
A
Hoechst GFP EdU
control
TMEM25 sh1
TMEM25 sh1
+
ARHGAP11B
B
n.s.
**
**
25
20
15
10
5
0
EdU+GFP+/GFP+(%)
control
TMEM25 sh1
TMEM25 sh1
+
ARHGAP11B

Figure 9. Inhibition of NPC proliferation by *TMEM25* knockdown and rescue by overexpression of *ARHGAP11B*

(A) Representative images of the NPCs stained for GFP (green) and EdU (red) in control, knockdown of *TMEM25,* and knockdown of *TMEM25* and overexpression of *ARHGAP11B*. Nuclei were stained with Hoechst (blue). (B) Quantification of EdU+GFP+ relative to GFP+ cells in (A). N = 3; Scale bar = 100um; **p < 0.01, n.s.: not significant.

Figure 10

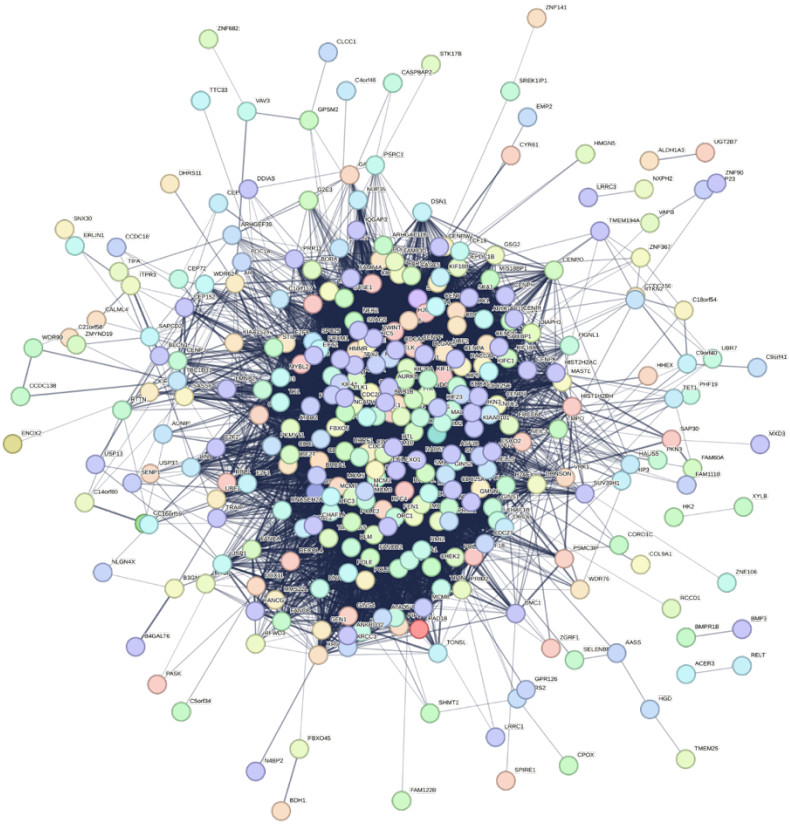

Figure 10. Protein-protein interaction network of downregulated genes in knockdown *TMEM25* NPCs

Figure 11

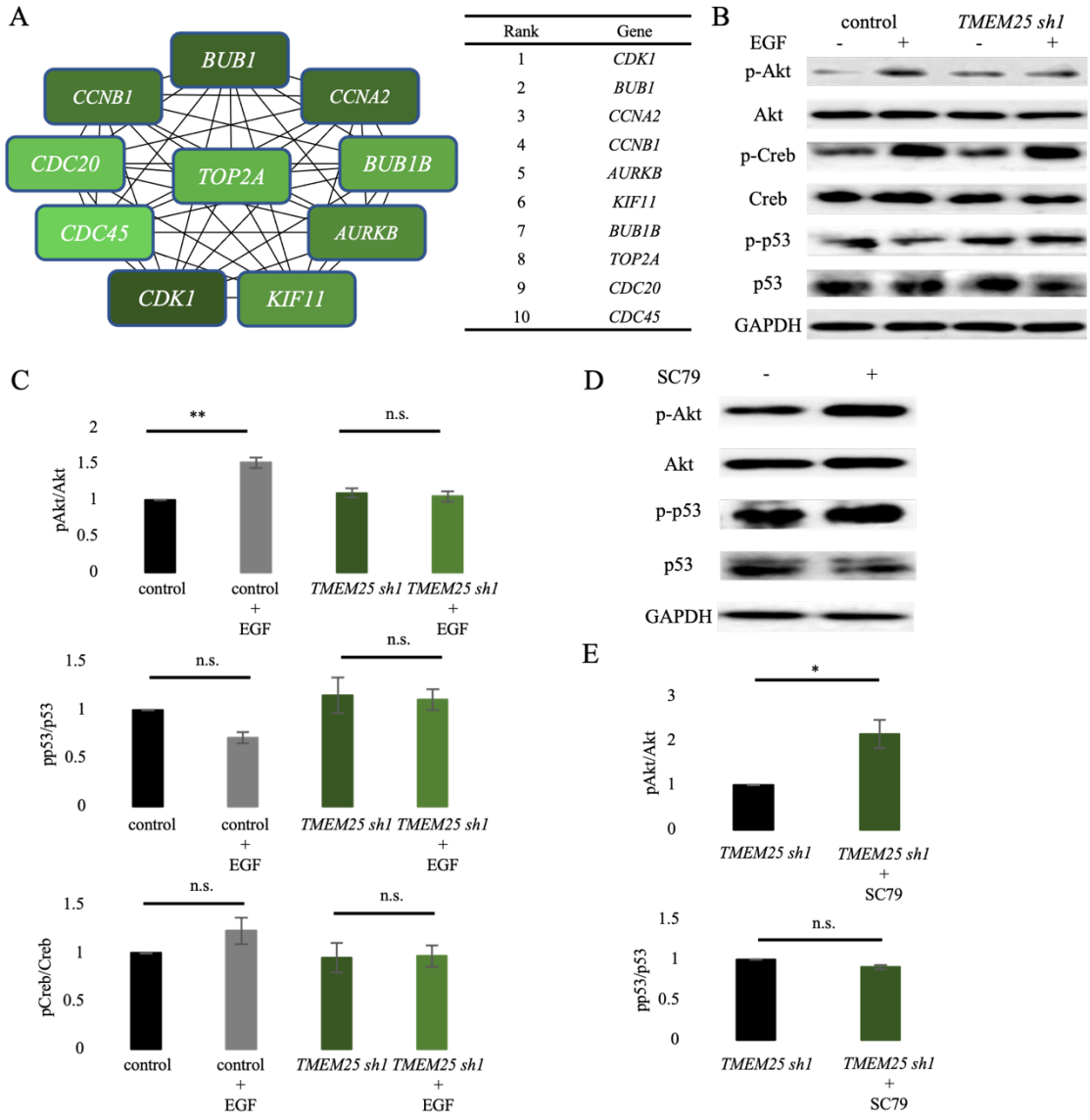
A
BUB1
CCNB1
CCNA2
CDC20
TOP2A
BUB1B
CDC45
AURKB
CDK1
KIF11
Rank
Gene
1 CDK1
2 BUB1
3 CCNA2
4 CCNB1
5 AURKB
6 KIF11
7 BUB1B
8 TOP2A
9 CDC20
10 CDC45
B
control
TMEM25 sh1
EGF
p-Akt
Akt
p-Creb
Creb
p-p53
p53
GAPDH
C
pAkt/Akt
pp53/p53
pCreb/Creb
control
control + EGF
TMEM25 sh1
TMEM25 sh1 + EGF
n.s.
**
D
SC79
E
TMEM25 sh1 + SC79
*

Figure 11. *TMEM25* regulates cell cycle via Akt/CDK1-CCNB1 pathway in NPCs

(A) Protein-protein interaction network of top 10 downregulated genes ranked by Degree and MNC algorithms in *TMEM25*-knockdown NPCs. (B) Immunoblot analysis of phospho-Akt, phospho-Creb and phospho-p53 in whole cell lysates from growth factor-starved sh*TMEM25* or control cells treated with EGF 20 min. (C) The ratio of phospho-Akt expression to total Akt, phospho-p53 expression to total p53 and phospho-Creb expression to total Creb in Fig.11B. (D) Immunoblot analysis of phospho-Akt and phospho-p53 in whole cell lysates from sh*TMEM25* cells treated with SC79 or DMSO. (E) The ratio of pAkt expression to total Akt in Fig.11D. N = 3; *$p < 0.05$, **$p < 0.01$, n.s.: not significant.

Figure 12

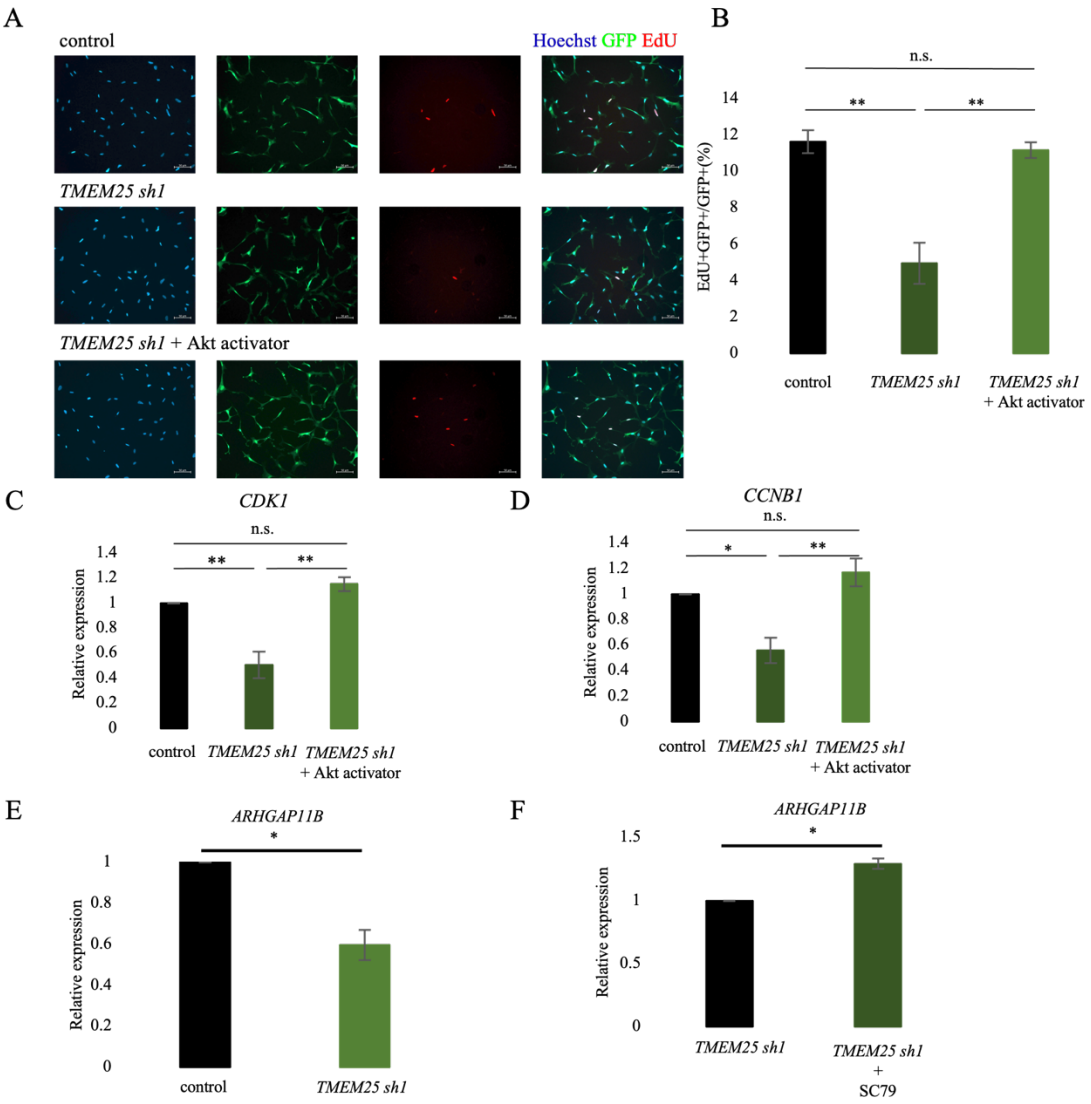
A
control
Hoechst GFP EdU
TMEM25 sh1
TMEM25 sh1 + Akt activator
B
n.s.
**
**
EdU+GFP+/GFP+(%)
14
12
10
8
6
4
2
0
control
TMEM25 sh1
TMEM25 sh1 + Akt activator
C
CDK1
n.s.
**
**
Relative expression
1.4
1.2
1
0.8
0.6
0.4
0.2
0
control
TMEM25 sh1
TMEM25 sh1 + Akt activator
D
CCNB1
n.s.
*
**
Relative expression
1.4
1.2
1
0.8
0.6
0.4
0.2
0
control
TMEM25 sh1
TMEM25 sh1 + Akt activator
E
ARHGAP11B
*
Relative expression
1
0.8
0.6
0.4
0.2
0
control
TMEM25 sh1
F
ARHGAP11B
*
Relative expression
1.5
1
0.5
0
TMEM25 sh1
TMEM25 sh1 + SC79

Figure 12. The expression levels of *CDK1*, *CCNB1* and *ARHGAP11B* were recovered after Akt activation

(A) Representative images of the NPCs stained for GFP (green) and EdU (red) in control, *TMEM25*-knockdown NPCs and *TMEM25*-knockdown NPCs treated with SC79. Nuclei were stained with Hoechst (blue). (B) Quantification of EdU+GFP+ to GFP+ cells in (A). (C and D) Quantification of the mRNA level of *CDK1* and *CCNB2* in *TMEM25*-knockdown NPCs treated with SC79. (E) Quantification of the mRNA level of *ARHGAP11B* after knockdown of *TMEM25*. (F) Quantification of the mRNA level of *ARHGAP11B* after knockdown of *TMEM25* and treatment with SC79. N = 3; Scale bar = 50 um; *p < 0.05, n.s.: not significant.

Figure 13

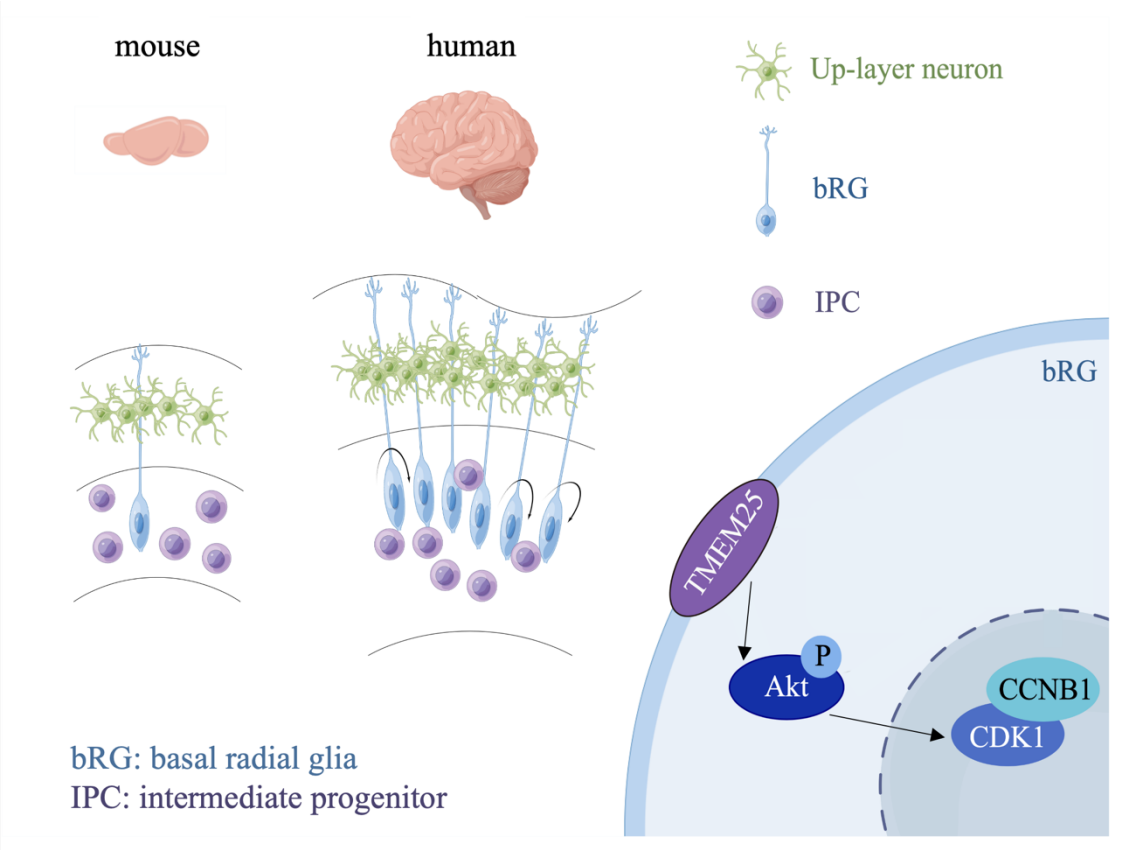
mouse
human
Up-layer neuron
bRG
IPC
bRG
TMEM25
P
Akt
CCNB1
CDK1
bRG: basal radial glia
IPC: intermediate progenitor

Figure 13. Proposed model for the role of *TMEM25* in cortical development.

High level of *TMEM25* expression promotes *CDK1/CCNB1* expression through activating Akt phosphorylation. This process promotes generation of basal radial glia to increase the density of upper-layer neurons in human cortical development.

Table 1 The list of primers used in this study

pLEMPRA_*TMEM25* Fw	CGGGAATTCCATGGCGCTGCCTCCAGGCCC
pLEMPRA_*TMEM25* Rv	TTAGGCGCGCCGCTCAGAGCCAGATCTCATCAC
pLEMPRA_*Tmem25* Fw	CGGGAATTCCATGGAATTGCCTCTAAGCCA
pLEMPRA_*Tmem25* Rv	TTAGGCGCGCCGCTCAGAGCCAAATCTCATCAC
sh *TMEM25*_1	GCAATTCAAGCCAGAGATTGC
sh *TMEM25*_2	GGGAGTTGGAGCCACAAATAG
qPCR *TMEM25* Fw	CCCGGCACCCATCTCTGATA
qPCR *TMEM25* Rv	GCTGGTTTCACTGCTCTGGA
qPCR *SOX2* Fw	TGGACAGTTACGCGCACAT
qPCR *SOX2* Rv	CGAGTAGGACATGCTGTAGGT
qPCR *KI67* Fw	ACGCCTGGTTACTATCAAAAGG
qPCR *KI67* Rv	CAGACCCATTTACTTGTGTTGGA
qPCR *CDK1* Fw	AAACTACAGGTCAAGTGGTAGCC
qPCR *CDK1* Rv	TCCTGCATAAGCACATCCTGA
qPCR *CCNB1* Fw	AATAAGGCGAAGATCAACATGGC
qPCR *CCNB1* Rv	TTTGTTACCAATGTCCCCAAGAG
qPCR *GAPDH* Fw	ACCACAGTCCATGCCATCAC
qPCR *GAPDH* Rv	TCCACCACCCTGTTGCTGTA
qPCR *ARHGAP11B* Fw	ACGCAGAAAAGAAGGGCGT
qPCR *ARHGAP11B* Rv	AAAGCCTTCCAGTGATGGAGT